Volume 13-Issue 6 (2024)

Journal of Transportation Science and Technology

Journal homepage: https://tapchicongnghegtvt.vn

Numerical simulation of horizontal rigid submarine landslide generated tsunami using FLOW-3D HYDRO model

Pham Van Khoi[1], Nguyen Thi Hong Hanh[1], Vu Van Nghi[2,*]

[1]*Faculty of Civil Engineering, Vietnam Maritime University*
[2]*Institute of Civil Engineering, University of Transport Ho Chi Minh City*

Keywords:
Rigid landslide
Submarine landslide
Tsunami
Numerical simulation
FLOW-3D HYDRO

ABSTRACT

This study presents a comprehensive numerical simulation of tsunamis generated by horizontal rigid submarine landslides using the FLOW-3D HYDRO model. Submarine landslides are critical geo-hazards that can trigger destructive tsunamis, posing severe risks to coastal communities. Unlike deformable landslides, rigid landslides maintain structural integrity, transferring energy more efficiently into the water column and producing distinctive, high-amplitude waves. The FLOW-3D HYDRO model, with its advanced capability to simulate multiphase flows and solid-fluid interactions, is used to explore these dynamics, focusing on the effects of slide velocity, slope angle, and water depth. Experimental data are used to validate the model, confirming its accuracy in reproducing observed wave dynamics. The results reveal that horizontal rigid submarine landslides generate waveforms with rapid onset and high initial amplitudes, which intensify near the shore. This research underscores the importance of high-resolution modeling to improve tsunami hazard assessments, especially for near-field events with limited early-warning timeframes. The insights from this study contribute to the development of more reliable early-warning systems and better-informed coastal defense strategies for mitigating tsunami impacts.

1. Introduction

Submarine landslides are critical geo-hazards capable of generating destructive tsunamis. Such events occur when large sediment masses displace underwater, transferring kinetic energy to the overlying water column, resulting in wave formation. Compared to earthquake-generated tsunamis, landslide-induced tsunamis can exhibit high wave heights over localized areas, posing significant risks to coastal

* Van Nghi Vu. Institute of Civil Engineering, Civil and Environmental Sustainable Development Research Group (CESD), University of Transport Ho Chi Minh City.
Email: nghi.vu@ut.edu.vn

https://www.doi.org/10.55228/JTST.13(6).57-66
Recieved: October 01, 2024,; Recieved in revised:October 25, 2024; Accepted: November 02, 2024
Available online: November 15, 2024
pISSN: 1859-4263; eISSN: 3030-4261

communities. Events like the 1998 Papua New Guinea tsunami exemplify this hazard, where a submarine landslide, triggered by a moderate earthquake, resulted in waves over 15 meters high and significant loss of life [1], [2]. Roger et al. [3] emphasized the difficulties in hazard identification and prediction. The author pointed out that landslide-generated tsunamis are more complex than earthquake-induced ones. Submarine landslides typically generate highly directional waves with short travel times, complicating the deployment of early warning systems [4]. This specificity makes probabilistic tsunami hazard assessments challenging but essential for risk management and planning [5].

One of the key challenges in understanding this hazard lies in its variability. Landslides can be triggered by multiple mechanisms, including seismic activity, rapid sediment loading, or climatic changes. The work by Whittaker et al. [6] emphasizes the importance of integrating bathymetric and seismic data to improve landslide detection and tsunami hazard modeling. Jing et al. [7] further highlight the role of numerical simulations in assessing the potential impacts of submarine landslides. The author shows how accurate modeling can mitigate risks through early-warning systems. Despite technological advancements, significant gaps remain in hazard assessment, especially in regions with sparse geological and bathymetric data [8]. Rigid submarine landslides involve the coherent displacement of relatively intact sediment or rock blocks, moving downslope as a single unit. Unlike deformable landslides, where sediments fragment and disperse, rigid slides maintain structural integrity throughout their motion. This difference has a significant impact on tsunami generation. Rigid landslides generally transfer energy more efficiently into the water column, resulting in higher initial wave amplitudes compared to softer, deformable slides [7], [9]. Their waveforms are sharper and more abrupt, often producing stronger near-field tsunami effects that pose an immediate hazard to coastal areas near the source [10].

Empirical data and numerical models have proven essential in accurately predicting tsunami behavior. Studies such as those by Whittaker et al. [6] and Kirby et al. [11] have demonstrated the importance of using high-resolution numerical tools to capture the complex dynamics associated with rigid landslides. These tools allow researchers to simulate the full lifecycle of a tsunami, from the initial displacement caused by the landslide to the wave propagation and coastal inundation phases. For instance, Jing et al. used smoothed particle hydrodynamics (SPH) models to replicate the generation and evolution of tsunami waves, providing essential insights into the relationship between slide mechanics and wave characteristics.

The FLOW-3D HYDRO model is a powerful computational tool for simulating free surface flows and solid-fluid interactions, with applications in tsunami modeling. The model's ability to handle multiphase flows and non-Newtonian dynamics is a significant advantage. This capability makes it particularly effective for studying submarine landslides and the generated tsunamis [8]. One of FLOW-3D HYDRO's strengths is its capacity to replicate complex phenomena such as sediment-fluid coupling and landslide motion along inclined planes. By employing FLOW-3D HYDRO, researchers can predict tsunami behavior, including wave heights, arrival times, and

inundation patterns. Studies like those by Jing et al. [7] and Whittaker et al. [9] emphasize the importance of accurate numerical tools for refining hazard models. FLOW-3D HYDRO's versatility allows researchers to analyze various scenarios, which is essential for validating tsunami generation mechanisms and assessing risk. This research leverages the model to simulate rigid submarine landslides and investigate their velocity profiles, providing insights that can improve hazard mitigation strategies.

This study aims to explore the generation and propagation of tsunamis caused by horizontal rigid submarine landslides. Through the use of FLOW-3D HYDRO, the research offers a deeper understanding of how horizontal rigid landslides influence wave dynamics, ultimately helping to develop better warning systems and coastal defense strategies.

2. Model description

In this section, the water wave module and the rigid body general moving object (GMO) model are introduced to clearly understand the strength of the FLOW-3D HYDRO model [12].

2.1. Water wave module

The water wave module uses the framework of Navier-Stokes equations. The continuity and momentum equations are given by:

$$\nabla \cdot \left(A\mathbf{u} \right) = 0 \tag{1}$$

$$\frac{\partial \mathbf{u}}{\partial t} + \frac{1}{V_F}\nabla \cdot (A\mathbf{u}\mathbf{u}) = -\frac{1}{\rho}\nabla \cdot p + G + f_v \tag{2}$$

Where $\nabla = \left(\partial/\partial x, \partial/\partial y, \partial/\partial z \right)$ is the gradient operator, A is the area fraction for the water in the mesh of a Cartesian coordinate system and is the volume fraction for water, V_F is the flow velocity in the x-, y-, z-direction; t is the time-dependence variable; ρ is the water density; p is the pressure; G is the body acceleration; f_v is the viscous acceleration. By using the famous volume of fluid (VOF) method, the free surface transportation equation between water and air is defined as:

$$\frac{\partial V_{\mathrm{w}}}{\partial t} + \frac{1}{V_{\mathrm{F}}}\nabla \cdot \left(V_{\mathrm{w}} A\mathbf{u} \right) = 0 \tag{3}$$

Where V_{w} is the water volume fraction in the cell of a free surface, and $V_{\mathrm{w}} = 0$, $0 < V_{\mathrm{w}} < 1$ and $V_{\mathrm{w}} = 1$ control the different phases of air, interface, and water, respectively. The turbulence model is applied for solving the dynamic viscosity μ using $k-\varepsilon$, giving the two equations as:

$$\frac{\partial k}{\partial t} + \frac{1}{V_{\mathrm{F}}}\left(uA_x \frac{\partial k}{\partial x} + vA_y \frac{\partial k}{\partial y} + wA_z \frac{\partial k}{\partial z} \right) = P_T + G_T + D_k - \varepsilon \tag{4}$$

$$\frac{\partial \varepsilon}{\partial t} + \frac{1}{V_{\mathrm{F}}}\left(uA_x \frac{\partial \varepsilon}{\partial x} + vA_y \frac{\partial \varepsilon}{\partial y} + wA_z \frac{\partial \varepsilon}{\partial z} \right) = \frac{C_{1\varepsilon}\varepsilon}{k}\left(P_T + C_{3\varepsilon}G_T \right) + D_\varepsilon - C_{2\varepsilon}\frac{\varepsilon^2}{k} \tag{5}$$

Where P_T is the turbulent kinematic energy production; G_T is the buoyancy production term; D_k and D_ε are the diffusion terms; and $C_{1\varepsilon}, C_{2\varepsilon}, C_{3\varepsilon}$ are constants.

2.2. General moving object module

The general moving object (GMO) module uses the following motion equation to describe a rigid body moving in the domain:

$$\mathbf{x}_s = \left[\mathrm{R}\right]\cdot\mathbf{x}_b + \mathbf{x}_G \tag{6}$$

Where $\mathbf{x}_s$ and $\mathbf{x}_b$ are the position vectors of a point in space and body system, respectively, $\mathbf{x}_G$ is the position vector of mass center in space system, and $\left[\mathrm{R}\right]$ is an orthogonal coordinate transformation tensor. Using those position vectors, the rigid body movement properties (e.g., velocity) can be determined in the model.

3. Numerical simulations

3.1. Numerical setup

In this section, the present simulations of the FLOW-3D HYDRO model are verified using the experimental data of Whittaker [1], [6], which were recently used to validate the analytical and other numerical models [7], [8]. This physical experiment showed the underwater rigid elliptic body moving in the horizontal plane as shown in Figure 1.

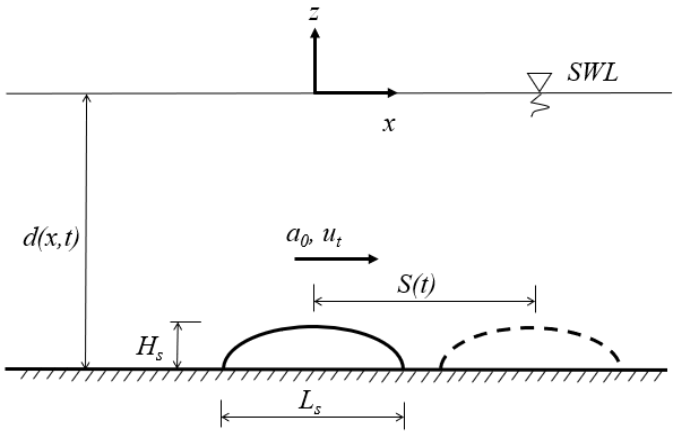

Figure 1. Schematic of underwater rigid elliptic body in a horizontal plane.

In Figure 1, the underwater rigid elliptic body had a constant shape with the length of L_s and the height of H_s, while the water depth $d(x, t)$ changed in space and time when the body moved. It caused the water response at the still water level (SWL), and the tsunami waves generally occurred.

In the physical experiment, two rigid body parameters, H_s, L_s were fixed, and three parameters, a_0, ut, and d_0 were changed. Where a_0 was the rigid body acceleration, ut was the rigid body terminal velocity, and d_0 was the constant water depth without rigid body height influence. The value of a_0 represented the property of rigid body motion, and the value of ut represented the strength of rigid body motion. Then, Whittaker et al. [6] grouped those changed values into three dimensionless parameters as follows:

$$\lambda = \frac{a_0}{g},\ Fr = \frac{u_t}{\sqrt{gd_0}},\ \mu = \frac{d_0}{L_s} \tag{7}$$

Where λ was the dimensionless landslide acceleration, Fr was the Froude number and μ was the ratio between the water depth and the landslide length (dispersion parameter). The first two parameters represented the rigid body motion, and the last parameter represented the dispersion property of the water wave mechanics. Finally, g is the gravitational acceleration. In the numerical experiment, the water depth changes in space and time is defined as follows:

$$d(x,t) = d_0 - H_s\left[1-\left(\frac{2\left(x-S(t)\right)}{L_s}\right)^4\right],\quad -\frac{L_s}{2}+S(t) < x < \frac{L_s}{2}+S(t) \tag{8}$$

Where *S(t)* is the rigid body motion, which is described as follows:

$$S(t)=\begin{cases}\frac{1}{2}a_0t^2, & 0\le t\le t_1\\ \frac{1}{2}a_0t_1^2+u_t(t-t_1), & t_1<t\le t_2\\ \frac{1}{2}a_0t_1^2+u_t(t_2-t_1)+u_t(t-t_2)-\frac{1}{2}a_0(t-t_2)^2, & t_2<t\le t_3\\ \frac{1}{2}a_0t_1^2+u_t(t_2-t_1)+u_t(t_3-t_2)-\frac{1}{2}a_0(t_3-t_2)^2, & t>t_3\end{cases} \quad (9)$$

At each time step, time values are defined as:

$$t_1=\frac{u_t}{a_0}, t_2=t_1+2, t_3=t_2+t_1 \quad (10)$$

It means that in the physical experimental mechanism, the velocity accelerates from 0 to *ut* in t_1 second. The constant value of ut is kept for 2 seconds before decelerating to 0 in t_1 seconds [6]. This procedure is shown in the velocity profile in Figure 2.

Depending on a_0, *ut* and d_0 values, 24 experimental cases were made by Whittaker [1], but in this verified application, only three cases of run 21, run 23, and run 12 (shown in Table 1) are employed to verify the submarine rigid landslide-generated waves using the FLOW-3D HYDRO model. These three testing cases are chosen to investigate the motion and dispersion properties of the rigid body and water waves, respectively.

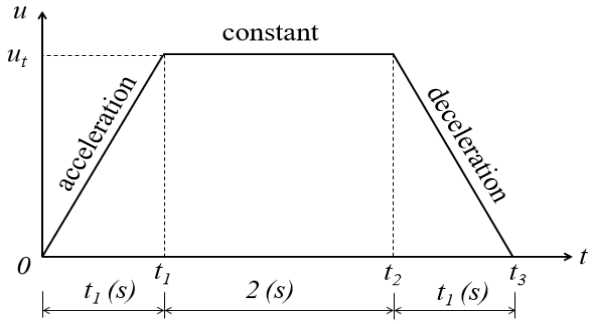

Figure 2. Underwater rigid elliptic body velocity profile for test cases.

Table 1. Parameters of 3 test cases.

Parameters	Case run 21	Case run 23	Case run 12
λ	0.153	0.153	0.102
Fr	0.125	0.375	0.500
μ	0.35	0.35	0.7
a_0 (m/s²)	1.5	1.5	1.0
d_0 (m)	0.175	0.175	0.35
ut (m/s)	0.164	0.491	0.926
t_1 (s)	0.109	0.327	0.926
t_2 (s)	2.109	2.327	2.926
t_3 (s)	2.218	2.654	3.852

In Table 1, the values of λ, *Fr* and μ are computed by the values of a_0, ut and d_0 using equation (7), and the values of t_1, t_2, and t_3 are computed by the values of a_0, *ut* using equation (10). We only increase the value of *ut* from 0.164 m/s to 0.491 m/s, which results in the *Fr* number of 0.375 in the case of run 23 compared to the *Fr* number of

0.125 in the case of run 21. While the λ value of 0.153 and the μ value of 0.35 are not changed. In the case of run 12, we increase the values of d_0 as well as ut and decrease the value of a_0, which results in the increases in the *Fr* number from 0.375 to 0.5 as well as the dispersion parameter μ from 0.35 to 0.7 and the reduction of dimensionless landslide acceleration λ from 0.153 to 0.102. Those experiments were conducted in a flume of length 14.66 m, width 0.25 m, and available depth 0.5 m. The rigid elliptic body had a length of L_s = 0.5 m, a width of W_s = 0.25 m, and a thickness of H_s = 0.026 m, and connected to the mechanical system beneath the flume floor. Finally, the free surface elevations were captured by the laser-induced fluorescence (LIF) technique [6].

In the numerical experiment, the FLOW-3D HYDRO model can be configured to accurately simulate the rigid submarine landslide movements in the GMO technique using the time and velocity values from 3 test cases in Table 1 and Figure 2. The water surface elevations, which can be easily analyzed using an appropriate data tool, are tracked using the VOF technique. The computational domain is established as the physical domain. Boundary conditions are set: the left and right boundaries allow water to pass through, the upper boundary is set to air pressure at 101,325 Pa, the lower boundary is defined as a wall, and both side boundaries are set to symmetry. A grid size of 0.005 m is used to achieve high resolution in the numerical domain. These settings help save simulation time and yield the best results.

3.2. Numerical results

The comparisons between present simulations and experimental data are shown in Figure 3, Figure 4, and Figure 5 of the test cases of runs 21, 23, and 12, respectively. Generally, the present simulations show good agreement with the experimental data. The FLOW-3D HYDRO model can accurately simulate the rigid submarine landslide-induced tsunami problem.

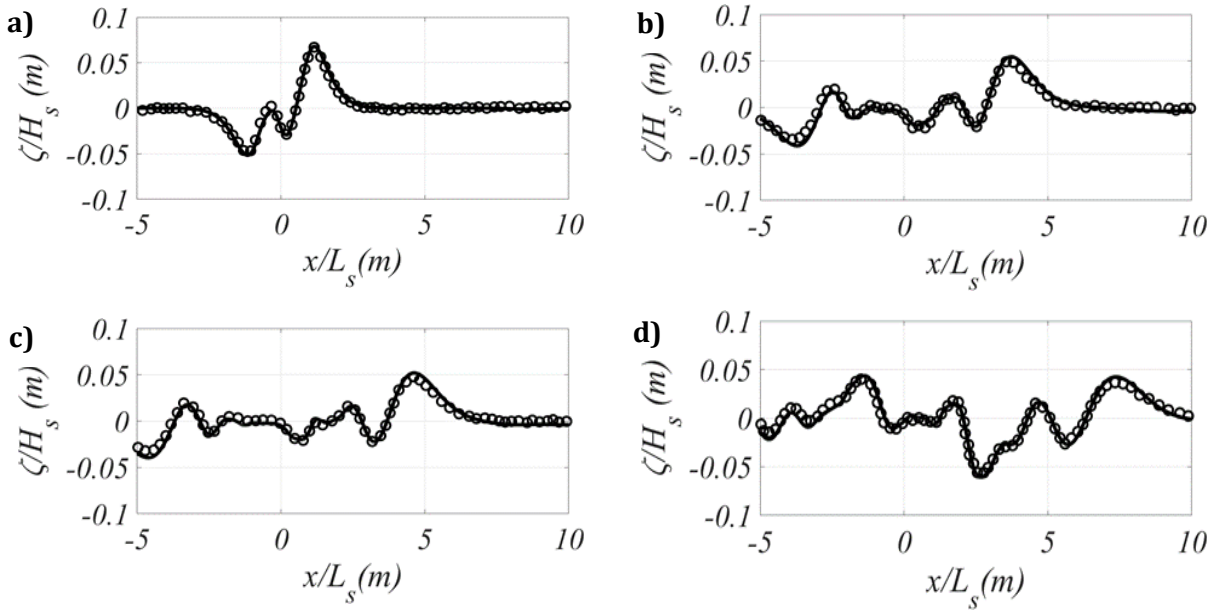

Figure 3. Comparison of present simulations (solid lines) with experimental data (circles) in case of run 21 at (a) t = 0.614 s, (b) t = 1.686 s, (c) t = 2.043 s, (d) t = 3.113 s.

In the next case, run 23, due to the increase only in submarine landslide speed in the *Fr* parameter from 0.125 to 0.375, the maximum wave heights increase approximately five times larger than those of the case of run 21, as shown in Figure 4. In comparison, the present results predict well the wave heights and wave trend with minor complexity, especially at instant time t = 3.113 s just after the terminal time of t = 2.654 s of the submarine landslide body.

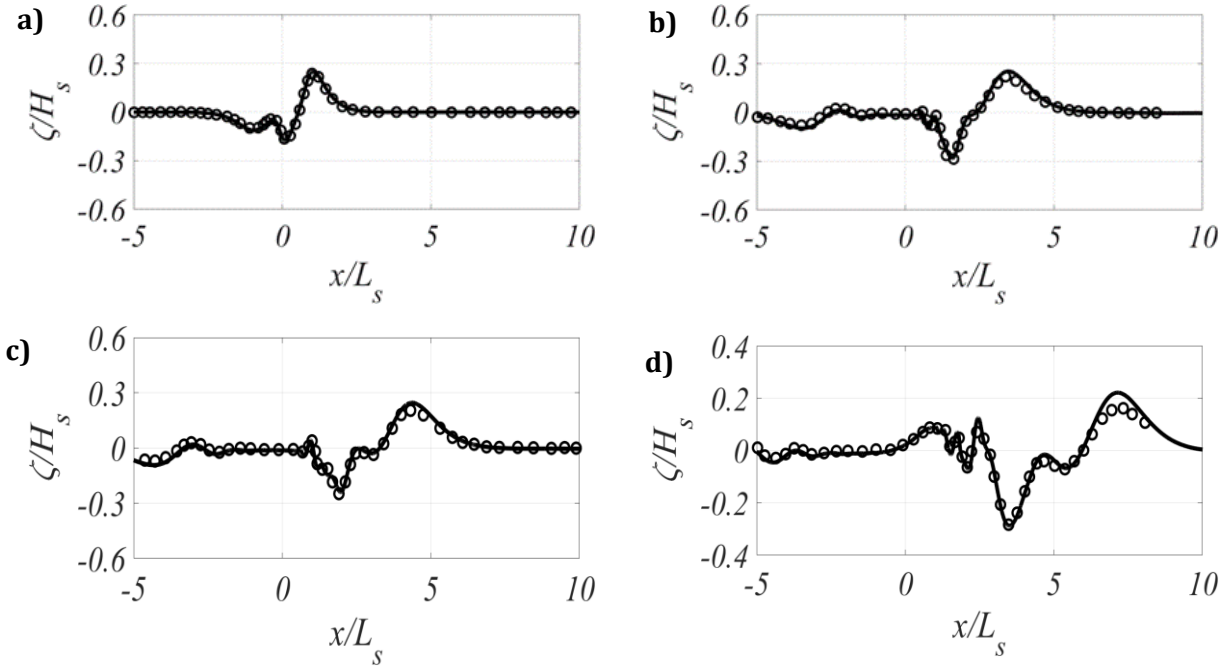

Figure 4. Comparison of present simulations (solid lines) with experimental data (circles) in case of run 23 at (a) t = 0.614 s, (b) t = 1.686 s, (c) t = 2.043 s, (d) t = 3.113 s.

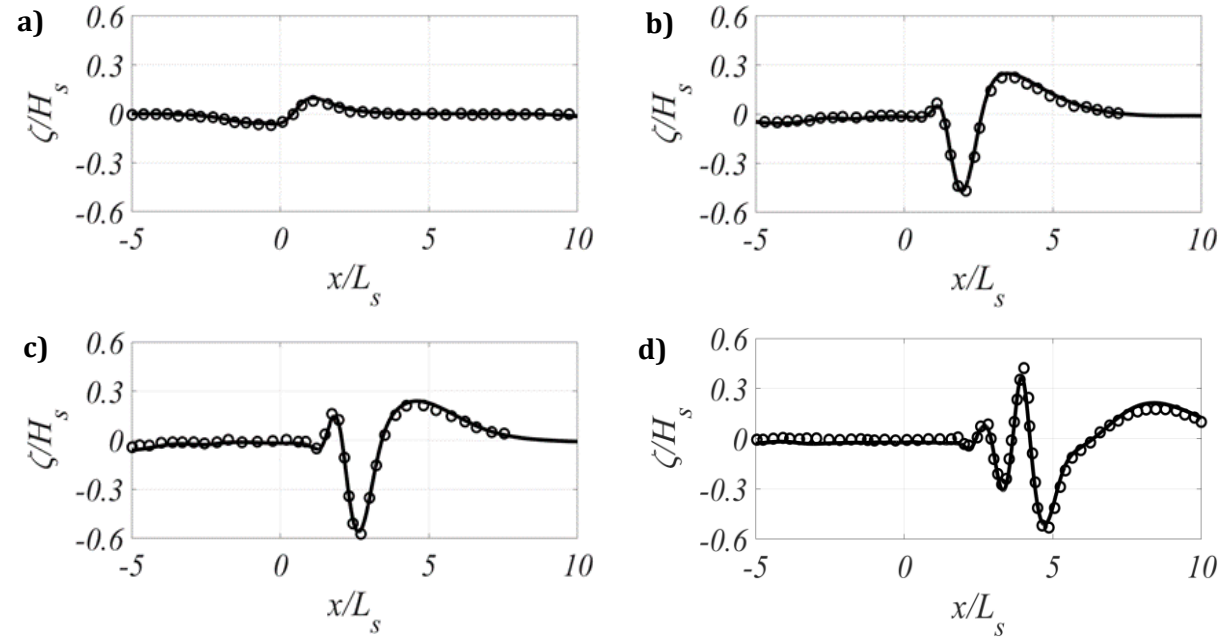

Figure 5. Comparison of present simulations (solid lines) with experimental data (circles) in case of run 12 at (a) t = 0.614 s, (b) t = 1.686 s, (c) t = 2.043 s, (d) t = 3.113 s.

The next complicated case is the case of run 12. It has not only the reduction of the landslide acceleration parameter λ from 0.153 to 0.102 but also the increases of both

the landslide speed parameter *Fr* number from 0.375 to 0.500 and dispersion property μ from 0.35 to 0.70. Until now, almost all numerical models [7], [10] cannot well predict this experimental data, especially in terms of wave heights.

However, the present results show good agreements with the measured data, even the wave heights at 4 instant times as shown in Figure 5. In this case, the difference in the motion is the submarine landslide body being not yet stopped (t_3 = 3.852 s) at the final instant time t = 3.113 s. Therefore, the wave shapes are simpler compared to those in the first two cases.

4. Discussion

The relationship between slide velocity, slope angle, and wave amplification can be understood through the way the landslide interacts with the water. Faster slides displace more water in a shorter time, leading to a sharper, more energetic wave.

The higher the velocity, the greater the initial energy transfer, which intensifies the wave. Similarly, when the slope angle increases, the landslide moves more vertically, causing a more sudden disturbance in the water. This steeper slope results in a more efficient conversion of the slide's potential energy into wave energy, producing larger waves. These findings align with Jing et al.'s observations that wave amplitude grows with both slide acceleration and slope steepness. A key observation from this study highlights the critical role of bathymetry in wave amplification, as the generated waves interact with varying seabed slopes, reinforcing observations by Kirby et al. [11].

This insight is valuable for understanding tsunami risk in regions with complex underwater topography. Additionally, the study by Tarwidi et al. [10] suggests that rigid landslides can amplify wave energy as they approach shallow coastal zones, heightening the tsunami's destructive potential nearshore. Overall, these results underscore the importance of high-resolution numerical models like FLOW-3D HYDRO in assessing rigid landslide-induced tsunami hazards, offering practical implications for early-warning systems and coastal planning efforts.

5. Conclusion

This study examined the tsunami-generating potential of horizontal rigid submarine landslides using the FLOW-3D HYDRO model. By focusing on horizontal rigid body motion, we aimed to understand how these types of landslides transfer energy into the water column, leading to the formation of high-amplitude tsunami waves. Unlike deformable landslides, which break apart and disperse, rigid landslides retain their structure, generating waves with sharp initial peaks and elevated amplitudes. These characteristics make rigid submarine landslides particularly hazardous in near-field regions, where the short travel time of tsunamis limits the effectiveness of early-warning systems.

The FLOW-3D HYDRO model demonstrated strong performance in simulating the dynamics of horizontal rigid landslides. Validation with experimental data showed that the model accurately reproduced key wave features, such as wave height, shape, and speed. Parameters like slide velocity were shown to significantly influence wave amplitude, with higher velocities producing stronger waves. This reinforces the model's potential for predicting tsunami impacts based on specific characteristics of the landslide. The findings emphasize the value of high-resolution

numerical modeling in assessing the risks associated with horizontal rigid submarine landslides.

FLOW-3D HYDRO's capabilities enable detailed simulation of these events, providing critical insights for improving tsunami hazard assessments and early-warning systems. By enhancing understanding of rigid landslide dynamics, this study offers practical benefits for coastal planning and disaster preparedness, particularly in regions vulnerable to sudden underwater landslide events.

Horizontal rigid submarine landslides pose a significant tsunami risk by generating powerful waves that can impact nearby coastlines with minimal advance warning. The FLOW-3D HYDRO model offers a reliable framework for accurately simulating these events, allowing for better-informed coastal defense strategies and risk management. Future research should focus on integrating real-time monitoring data and exploring variations in landslide characteristics to further improve model precision and applicability in tsunami prediction.

Contributions of authors in this article

Pham Van Khoi: Methodology, Data management, Formal analysis, Investigation, Validation, Visualization, Grant acquisition, Feedback on peer review, Writing – original manuscript. **Nguyen Thi Hong Hanh**: Data compilation, Investigation, Feedback on peer review, Writing – revised manuscript. **Vu Van Nghi**: Data compilation, Data analysis, Investigation, Verification, Feedback on peer review, Writing – original manuscript.

Declaration of competing interest and dedication to copyright

The authors declare the absence of any potential conflicts of interest from this study and affirm that the paper has not been previously published.

Data available

Data will be provided upon request.

References

[1] C. Whittaker, "Modelling of tsunami generated by the motion of a rigid block along a horizontal boundary," Ph.D. dissertation, Civil and Natural Resources Engineering, University of Canterbury, 2014.

[2] D. R. Tappin, "Submarine Landslides and Their Tsunami Hazard," *Annu. Rev. Earth Planet. Sci.*, vol. 49, pp. 551-578, 2021, doi: 10.1146/annurev-earth-063016-015810.

[3] J. H. M. Roger et al., "A review of approaches for submarine landslide-tsunami hazard identification and assessment," *Mar. Pet. Geol.*, vol. 162, Apr. 2024, Art. no. 106729, doi: 10.1016/J.MARPETGEO.2024.106729.

[4] C. B. Harbitz, F. Løvholt, and H. Bungum, "Submarine landslide tsunamis: how extreme and how likely?," *Nat. Hazards*, vol. 72, pp. 1341-1374, 2014, doi: 10.1007/s11069-013-0681-3.

[5] S. Yavari-Ramshe and B. Ataie-Ashtiani, "Numerical modeling of subaerial and submarine landslide-generated tsunami waves—recent advances and future challenges," *Landslides*, vol. 13, pp. 1325-1368, 2016, doi: 10.1007/S10346-016-0734-2.

[6] C. Whittaker, R. Nokes, and M. Davidson, "Tsunami forcing by a low Froude number landslide," *Environ. Fluid Mech.*, vol. 15, pp. 1215–1239, 2015, doi: 10.1007/S10652-015-9411-6/METRICS.

[7] H. Jing, G. Chen, C. Liu, W. Wang, and J. Zuo, "Dispersive effects of water waves generated by submerged landslide," *Nat. Hazards*, vol. 103, pp. 1917–1941, 2020, doi: 10.1007/S11069-020-04063-Z/METRICS.

[8] D. Tarwidi, S. R. Pudjaprasetya, and D. Adytia, "A reduced two-layer non-hydrostatic model for submarine landslide-generated tsunamis," *Appl. Ocean Res.*, vol. 127, Oct. 2022, Art. no. 103306, doi: 10.1016/J.APOR.2022.103306.

[9] C. N. Whittaker, R. I. Nokes, H. -Y. Lo, P. L. -F. Liu, and M. J. Davidson, "Physical and numerical

modelling of tsunami generation by a moving obstacle at the bottom boundary," *Environ. Fluid Mech.*, vol. 17, pp. 929-958, Oct. 2017, doi: 10.1007/S10652-017-9526-Z/METRICS.

[10] D. Tarwidi, S. R. Pudjaprasetya, and S. S. Tjandra, "A non-hydrostatic model for simulating weakly dispersive landslide-generated waves," Water, vol. 15, no. 4, 2023, Art. no. 652, doi: 10.3390/W15040652.

[11] J. T. Kirby et al., "Validation and inter-comparison of models for landslide tsunami generation," *Ocean Model.*, vol. 170, Feb. 2022, Art. no. 101943, doi: 10.1016/J.OCEMOD.2021.101943.

[12] FLOW-3D, "FLOW-3Da HYDRO." flow3d.com. Accessed: Sep. 20, 2024. [Online]. Available: https://www.flow3d.com/products/flow-3d-hydro/